Plasmon-pole approximation for semiconductor quantum-wire electrons

S. Das Sarma, E. H. Hwang, and Lian Zheng
Department of Physics, University of Maryland, College Park, Maryland 20742-4111
(Received 28 May 1996)

We develop the plasmon-pole approximation for an interacting electron gas confined in a semiconductor quantum wire. We argue that the plasmon-pole approximation becomes a more accurate approach in quantum-wire systems than in higher-dimensional systems because of severe phase-space restrictions on particle-hole excitations in one dimension. As examples, we use the plasmon-pole approximation to calculate the electron self-energy due to the Coulomb interaction and the hot-electron energy relaxation rate due to LO-phonon emission in GaAs quantum wires. We find that the plasmon-pole approximation works extremely well as compared with more complete many-body calculations. [S0163-1829(96)04536-5]

I. INTRODUCTION

Recently, there has been an increasing interest[1] in semiconductor quantum-wire structures, where the motion of electrons is essentially restricted to be one dimensional. Technological progress has made it possible to fabricate[2] high quality quantum wires where only the lowest subband is populated by electrons, so that a truly one-dimensional interacting electron gas is realized. Much in the same way as quantum-well structures have generated tremendous activities in pure and applied research on two-dimensional electron systems, quantum-wire structures have created the potential for different device applications[1,3,4] and the opportunity to carry out experimental study on one-dimensional Fermi systems, where many theoretical predictions[5] can be tested. Because of the low dimensionality, properties of a quantum wire are very sensitive to electron-electron interaction effects.[5,6] Many experimentally relevant quantities need to be calculated by taking into account many-body interaction induced exchange-correlation effects. The standard perturbation theories, which have been developed for higher-dimensional electron systems, have been applied[6,7] to quantum-wire systems, and good agreement with experiments[2,8] are generally obtained. In this paper, we discuss the application of another well known many-body approach, the plasmon-pole approximation,[9,10] to quantum-wire systems. The motivation for this work is the observation that the collective plasmon excitation plays a more prominent role in a one-dimensional electron system compared with its higher-dimensional counterparts because single-particle electron-hole excitation continuum is severely restricted in one dimension due to energy-momentum conservation. Thus, the plasmon-pole approximation, besides having the obvious benefit of great simplicity, may work well for one-dimensional quantum wires in calculating exchange-correlation effects. To illustrate this point, we calculate the electron self-energy correction due to electron-electron Coulomb interaction and the electron energy relaxation rate due to electron LO-phonon Fröhlich interaction and compare the plasmon-pole approximation results with the corresponding full many-body calculations using the random-phase approximation (RPA).

The plasmon-pole approximation has been extensively employed[9–12] in calculating the electron self-energies of three- and two-dimensional systems. The results obtained from these calculations are in good semiquantitative agreement with the results of more sophisticated treatments—namely, the full RPA calculations, and with experimental results. A many-body interacting electron system has both collective plasmon excitations and single-particle electron-hole excitations.[13] The plasmon-pole approximation simplifies the many-body excitation spectrum by ignoring the particle-hole excitations and assigning the whole spectral weight, which is dictated by the f-sum rule,[13] to an effective collective plasmon excitation, which is assumed to be a real pole of the response function. This is, in general, a crude approximation for the actual dynamical response of the electron system, except in the long wavelength limit where the plasmon excitation exhausts all the spectral weight in a uniform system[13] by virtue of particle conservation. It is well known that in a one-dimensional system, the collective plasmon excitation plays a more prominent role because of phase space restriction on particle-hole excitations. In fact, the long wavelength RPA plasmon dispersion is exact in one-dimensional electron liquids up to the second order in wave vector in contrast to higher-dimensional systems.[14] It is, therefore, worthwhile to explore the possibility that the plasmon-pole approximation may actually work better in quantum-wire systems than in higher-dimensional systems. Our work is motivated by this purpose. We find that the one-dimensional phase-space restriction on the particle-hole excitations indeed increases the spectral weight of the plasmon excitation over a wide range of wave vectors in one-dimensional systems under conditions which are typical in GaAs-based quantum-wire samples, and the plasmon-pole approximation indeed works extremely well in calculating a variety of quantities in GaAs-based quantum-wire structures. We specifically apply the plasmon-pole approximation to two different problems: one involves the electron-electron Coulomb interaction and the other involves the polar electron LO-phonon Fröhlich interaction. In the first case, we calculate quasiparticle properties of the interacting electrons by taking into account the Coulomb interaction effects through the plasmon-pole approximation. In the second case, we calculate the hot-electron energy-loss rate via LO-phonon emission. We show that the plasmon-pole approximation

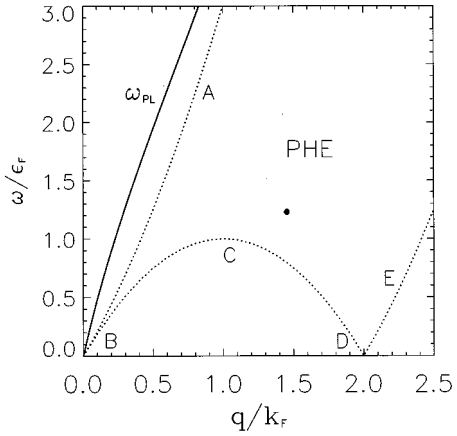

FIG. 1. Excitation spectrum of a one-dimensional electron gas in the RPA. Particle-hole excitations are confined within the phase space surrounded by the dotted line $ABCDE$. Plasmon excitation is represented by the solid line.

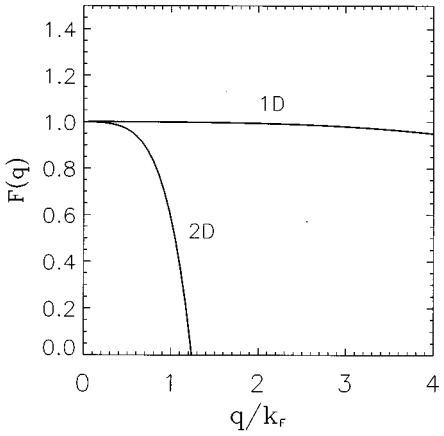

FIG. 2. Calculated RPA oscillator strengths of plasmon excitations of 1D quantum-wire and 2D quantum well electron systems. The input parameters are taken from GaAs-based materials: density $n=10^5$ cm^{-1} and lateral width $a=b=200$ Å for the quantum wire; density $n=1.6\times10^{11}$ cm^{-2} for a zero thickness purely 2D quantum well.

works well in both cases by giving results which are in good agreement with the corresponding RPA results, which are much more difficult computationally.

In Fig. 1, we show the elementary excitation spectrum of a one-dimensional electron system calculated within the RPA, where the particle-hole excitations are confined within the phase-space surrounded by the dotted-line $ABCDE$, and the plasmon excitation is represented by the solid line. In one dimension, the RPA plasmon dispersion has a simple analytical expression[7] (we set $\hbar=1$ throughout this paper),

$$\omega_q=\frac{A(q)E_+(q)-E_-(q)}{A(q)-1}, \tag{1}$$

where $E_\pm(q)=q^2/2m\pm k_Fq/m$ with m as electron mass and k_F the electron Fermi wave vector, $A(q)=\exp[q/\pi V_c(q)]$ with $V_c(q)$ as the electron-electron Coulomb interaction potential[16] of a quantum wire of finite lateral width. Unlike plasmon modes in higher dimensions, the RPA plasmon excitation in a quantum wire exists (i.e., is undamped) for all wave vectors $0\leqslant q<\infty$.

The most characteristic feature of the one-dimensional spectrum is that particle-hole excitations are prohibited from a large portion of the low energy phase space, the region below the dotted line BCD in Fig. 1. This restriction, which arises from the momentum-energy conservation, increases the dominance of plasmon excitations in a quantum wire compared with higher-dimensional systems. The situation is totally different in higher-dimensional systems,[13] where particle-hole excitations are allowed in the whole phase space between the dotted lines AB and DE in Fig. 1. For a quantitative measure of the relative importance of the plasmon excitation, we evaluate its oscillator strength within the RPA,

$$F(q)=-\frac{2m}{\pi nq^2}\int_0^\infty \omega S_{\rm PL}(q,\omega)d\omega, \tag{2}$$

where n is the average density of the electron gas, and the plasmon spectral weight is defined by [with the plasmon dispersion ω_q given by Eq. (1)]

$$S_{\rm PL}(q,\omega)=-\frac{\pi}{V_c(q)}\frac{1}{\left|\frac{\partial}{\partial\omega}{\rm Re}[\epsilon(q,\omega)]\right|}\delta[\omega-\omega_q].$$

In Fig. 2, we compare the oscillator strengths of plasmon excitation of a one-dimensional quantum wire with that of a two-dimensional quantum well (both obtained within the RPA). The plasmon oscillator strength in the quantum well drops quickly to zero at a critical wave vector, beyond which an undamped well-defined plasmon mode does not exist. The oscillator strength of the plasmon excitation in a quantum wire, on the other hand, extends well into the range of large wave vectors, decreasing slowly with increasing wave vector. Note that the $q\to0$ behavior of these curves, i.e., $F(q)=1$ for $q\to0$, is just a manifestation of the f-sum rule. The interesting point is that $F(q)\sim1$ in one dimension even for $q>k_F$. It is seen clearly that the plasmon dominance of the spectral weight is significantly increased in quantum-wire systems. Since the plasmon-pole approximation assumes that the excitation spectrum consists of no particle-hole excitations, but solely of a collective mode which exists for all values of wave vectors and possesses unit oscillator strength, it is easy to understand why the plasmon-pole approximation may work well in a quantum-wire system. The density-density response function of a quantum-wire electron system in the plasmon-pole approximation is given as

$$\chi_{\rm PP}(q,\omega)=\frac{\frac{n}{m}q^2}{\omega^2-\omega_q^2}. \tag{3}$$

By construction, $\chi_{PP}(q,\omega)$ in the above expression satisfies the f-sum rule and the static Kramers-Kronig relation.[13] Equation (3) is our plasmon-pole approximation model,[9–12] which we use to calculate quantum-wire many-body electronic properties.

In Secs. II and III, we apply the plasmon-pole approximation to the calculations of electron self-energy due to Cou-

lomb interaction and electron energy relaxation rate due to LO-phonon emission, respectively. A short summary in Sec. IV concludes our paper.

II. SELF-ENERGY AND SPECTRAL FUNCTION

The one-dimensional (1D) self-energy within the leading order GW approximation[15] neglecting vertex correction at $T=0$ is given by

$$\Sigma(k,\omega)=i\int \frac{dq\,d\omega'}{(2\pi)^2}W(q,\omega)G_0(k-q,\omega-\omega'), \quad (4)$$

where $G_0(k,\omega)$ is the Green's function for the noninteracting electron gas,

$$G_0(k,\omega)=\frac{\theta(|k|-k_F)}{\omega-\xi(k)+i0^+}+\frac{\theta(k_F-|k|)}{\omega-\xi(k)-i0^+}, \quad (5)$$

with $\xi(k)=k^2/2m-\mu$ (μ=chemical potential), and $W(q,\omega)$ is the dynamically screened Coulomb interaction, which is given by

$$W(q,\omega)=\frac{V_c(q)}{\epsilon(q,\omega)}. \quad (6)$$

Here $V_c(q)$ is the bare Coulomb interaction, which is logarithmically divergent in the 1D wave vector space. Thus, we use the more realistic finite width quantum-wire model, the fully approximated matrix element of which can be found in the literature.[16] $\epsilon(q,\omega)$ is the dielectric function, which describes the dynamical screening properties of the electron gas. The dynamically screened interaction $W(q,\omega)$ can be separated into an unscreened term which gives rise to the exchange part of the self-energy and another term which gives rise to the correlation part of the self-energy and involves coupling to density fluctuations,

$$W(q,\omega)=V_c(q)+V_c(q)\left[\frac{1}{\epsilon(q,\omega)}-1\right]. \quad (7)$$

The imaginary part of the second term is nonzero within the electron-hole continuum and along the plasmon dispersion line in the RPA. In the plasmon-pole approximation (PPA),[9–12] the second term is replaced by a coupling to the effective plasmon mode as described in Sec. I,

$$\mathrm{Im}\left[\frac{1}{\epsilon(q,\omega)}-1\right]=-\frac{\pi}{2}\frac{\omega_0^2}{\omega_q}\delta(\omega-\omega_q), \quad (8)$$

where the strength $\omega_0^2=(n/m)V_C(q)q^2$ is determined by the requirement that Eq. (8) satisfies the f-sum rule, and ω_q is the 1D plasmon dispersion which is exactly known within RPA (Ref. 7) [see Eq. (1)]. Unlike in 2D and 3D, where the exact analytic RPA plasmon dispersion is unknown so that the static RPA dielectric function $\epsilon(q,\omega=0)$ is used in obtaining the effective plasmon frequency ω_q, we use the analytically known 1D RPA plasmon dispersion given in Eq. (1). Note that any attempt to use the static RPA (similar to what is done in 2D and 3D PPA) in 1D PPA is not only unnecessary (because the 1D RPA plasmon dispersion is known analytically), but also incorrect because the 1D static RPA dielectric function has logarithmic zero temperature singularities due to a divergence at $q=2k_F$. Using the Kramer-Kronig relation, we have

$$\frac{1}{\epsilon(q,\omega)}-1=\frac{\omega_0^2}{\omega^2-\omega_q^2+i\delta}. \quad (9)$$

Within the PPA the self-energy can now be separated into a frequency independent exchange term and a correlation term

$$\Sigma(k,\omega)=\Sigma_{\mathrm{ex}}(k,\omega)+\Sigma_{\mathrm{cor}}(k,\omega), \quad (10)$$

where

$$\Sigma_{\mathrm{ex}}(k,\omega)=i\int \frac{dq\,d\omega'}{(2\pi)^2}V_c(q)G_0(k+q,\omega+\omega'), \quad (11)$$

and

$$\Sigma_{\mathrm{cor}}(k,\omega)=i\int \frac{dq\,d\omega'}{(2\pi)^2}V_c(q)\left[\frac{1}{\epsilon(q,\omega')}-1\right]\times G_0(k+q,\omega+\omega'). \quad (12)$$

The exchange energy $\Sigma_{\mathrm{ex}}(k,\omega)$ as well as the correlation energy Σ_{cor} within the full RPA theory has been calculated earlier by Hu and Das Sarma.[6] Using Eq. (9) in Eq. (12) and performing a frequency integration, the correlation part becomes

$$\Sigma_{\mathrm{cor}}=\int \frac{dq}{2\pi}\frac{V_c(q)\omega_{\mathrm{p}}^2}{2\omega_q}\left[\frac{\theta(k_F-|k+q|)}{\omega+\omega_q-\xi_{k+q}-i\delta}+\frac{\theta(|k+q|-k_F)}{\omega-\omega_q-\xi_{k+q}+i\delta}\right]. \quad (13)$$

The real and the imaginary parts of the Σ_{cor} are given by

$$\mathrm{Re}\Sigma_{\mathrm{cor}}(k,\omega)=\mathrm{P}\int \frac{dq}{2\pi}g(q)\left[\frac{\theta(k_F-|k+q|)}{\omega+\omega_q-\xi_{k+q}}+\frac{\theta(|k+q|+k_F)}{\omega-\omega_q-\xi_{k+q}}\right], \quad (14)$$

and

$$\mathrm{Im}\Sigma_{\mathrm{cor}}(k,\omega)=\pi\int \frac{dq}{2\pi}g(q)[\,\theta(k_F-|k+q|)\times\delta(w+w_q-\xi_{k+q})-\theta(|k+q|-k_F)\times\delta(\omega-\omega_q-\xi_{k+q})], \quad (15)$$

where $g(q)=V_c(q)\omega_0^2/(2\omega_q)$ and $\mathrm{P}\int$ indicates the principle value integral. >From the restrictions on the integration region arising from various θ and δ functions, we see that $\mathrm{Im}\Sigma_{\mathrm{cor}}$ is nonzero only for

$$\begin{aligned}&\omega_q(k_F-k)>\omega \quad \text{and} \quad -\omega_q(k_F+k)<\omega<\xi_k \quad \text{if } k\leqslant k_F,\\ &\xi_k>\omega \quad \text{and} \quad -\omega_q(k_F+k)<\omega<-\omega_q(k-k_F) \quad \text{if } k>k_F.\end{aligned} \quad (16)$$

Carrying out the integral over q, one obtains the imaginary part of the Σ_{cor}

$$\mathrm{Im}\Sigma_{\mathrm{cor}}(k,\omega)=\frac{1}{2}\sum_i\left[\frac{g(q_{+,i})\,\theta(k_F-|k+q_{+,i}|)}{|d\Omega_+(q_{+,i})/dq|}+\frac{g(q_{-,i})\,\theta(|k+q_{-,i}|-k_F)}{|d\Omega_-(q_{-,i})/dq|}\right], \quad (17)$$

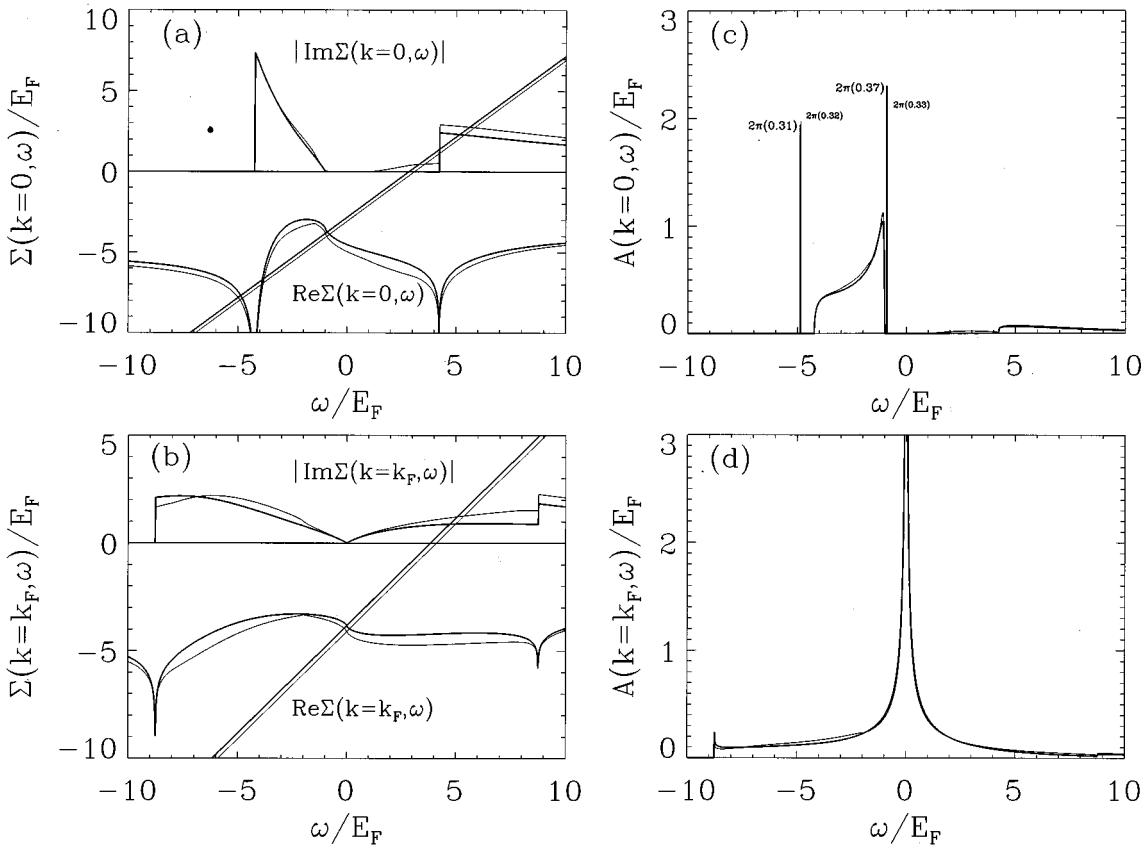

FIG. 3. (a), (b) Self-energy $\Sigma(k,\omega)$ and (c), (d) spectral function $A(k,\omega)$ as functions of the frequency ω for two fixed wave vectors $k=0$ [(a) and (c)] and k_F [(b) and (d)]. Thick (thin) lines correspond to the PPA (RPA) results. The vertical lines in (c) represent δ functions with the spectral weight given above the peaks. The straight lines in (a) and (b) are given by $\omega-\xi(k)-\mu$, and their intersections with Re$[\Sigma]$ indicate the solutions to Dyson's equation and correspond to quasiparticle peaks. $|\mathrm{Im}\Sigma|$ is plotted instead of ImΣ for visual clarity.

where $\Omega_{\pm}(q)=\omega\pm\omega_q-\xi_{k+q}$ and $q_{\pm,i}$ are zeros of $\Omega_{\pm}(q)$. From Eqs. (15) and (16) we know that Im$[\Sigma(k,\omega)]$ as a function of ω has finite discontinuities at $\omega=\pm\omega_q(k+k_F)$, the magnitude of which can be calculated from Eq. (17). For example, we have the magnitude $g(k_F)/[\partial\omega_q(k_F)/\partial q\pm k_F/m]$ at $\omega=\pm\omega_q(k_F)$ for $k=0$ and $(1/2)g(2k_F)/[\partial\omega_q(2k_F)/\partial q\pm k_F/m]$ at $\omega=\pm\omega_q(2k_F)$ for $k=k_F$. [See the numerically calculated values in Figs. 3(a) and (b).] A finite discontinuity in Im$[\Sigma]$ gives rise to a logarithmic singularity in Re$[\Sigma]$, which can be verified using the Kramers-Kronig relation. [See Figs. 3(a) and (b).]

In order to determine quasiparticle excitation energies one must solve the Dyson equation[15] which is given by

$$\omega+\mu=\xi(k)+\Sigma(k,\omega), \tag{18}$$

where μ is the chemical potential of the interacting electron gas, which is determined by setting $k=k_F$ and $\omega=0$ in the above equation. Once the self-energy $\Sigma(k,\omega)$ is known, the single-particle spectral function $A(k,\omega)$ is readily calculated. $A(k,\omega)$ contains important dynamical information about the system and is given by

$$A(k,\omega)=\frac{2|\mathrm{Im}\Sigma(k,\omega)|}{[\omega-\xi(k)-\mathrm{Re}\Sigma(k,\omega)]^2+[\mathrm{Im}\Sigma(k,\omega)]^2}. \tag{19}$$

It satisfies the sum rule

$$\int_{\infty}^{\infty}\frac{d\omega}{2\pi}A(k,\omega)=1, \tag{20}$$

which we verify to be satisfied within less than a percent in our numerical calculations.

Figure 3 shows the calculated self-energies and spectral functions as a function of frequency ω for $k=0$ (band edge) and $k=k_F$ (Fermi energy). The complete RPA results[6] (thin lines) are also shown for comparison with our PPA results. From the figures we can see that our PPA results are almost identical to the full RPA results.[6] In both calculation the parameters corresponding to GaAs are used: $m=0.07m_e$ (m_e is the free electron mass), $\epsilon_0=12.9$, $\epsilon_\infty=10.9$, and $\omega_{LO}=36.8$ meV. The well width of $a=100$ Å and the 1D electron density of $n=0.56\times10^6$ cm^{-1}, which corresponds to a Fermi energy $E_F\approx4.4$ meV and a dimensionless density parameter $r_s=4me^2/\pi k_F\epsilon_0=1.4$ with $k_F=\pi n/2$, are used in both calculation. In Figs. 3(a) and 3(b) the straight lines are given by $\omega-\xi(k)-\mu$, and their intersections with Re$[\Sigma]$ indicate the solutions to Dyson's equation and correspond to quasiparticle peaks. In the spectral function for $k=0$, we find

two undamped quasiparticle peaks. The strength ($2\pi\times 0.37$) of the regular quasiparticle (the first peak near $\omega=0$) within PPA is slightly higher than the corresponding RPA result ($2\pi\times 0.33$). The strength ($2\pi\times 0.31$) of the second peak, the so-called plasmaron peak, is nearly the same in the PPA as that in the RPA ($2\pi\times 0.32$). The low energy incoherent spectrum [$E_F<\omega<\omega_q(k_F)$] arising from the electron-hole continuum within RPA is transferred to the quasiparticle spectrum in the PPA, making the quasiparticle spectral weight slightly higher in the PPA than in the RPA. For $k=k_F$ we find that the quasiparticlelike peak at $\omega=0$ is not a strict δ-function peak, which means that the system within PPA has no true long-lived quasiparticles. This result is qualitatively the same as the RPA result, implying that there can be no true quasiparticles in one dimension. As $\omega\rightarrow 0$, the dominant contribution to Im[$\Sigma(k_F,\omega)$] within RPA comes from the plasmon excitation.[6] Therefore, the behavior of the spectral function near $\omega=0$ for $k=k_F$ shows exactly the same behavior for both the PPA and the RPA.

In 2D (Ref. 12) and 3D,[9,10] the quantitative differences between the results of plasmon-pole approximation and the random-phase approximation are comparable, and are considerably larger than what we find in our 1D calculations. In our 1D calculation, the agreement between the RPA and PPA self-energies is almost perfect. Since the 1D electron-hole continuum is strongly suppressed by the severe phase restriction due to energy-momentum conservation, the 1D plasmon is the dominant excitation which contributes to the electron self-energy, with the contribution from single-particle excitations being essentially negligibly small. In this paper, we provide an easy method for calculating the effects of correlation on the single-particle self-energy in one dimension. It should be fairly straightforward to extend the PPA self-energy calculation to more complicated experimentally relevant situations, such as finite temperatures and multisubband occupancies, with reasonable confidence of obtaining quantitatively accurate results. This is the main significance of our work.

III. ENERGY RELAXATION IN A QUANTUM WIRE

In this section, we apply the plasmon-pole approximation to a coupled electron-LO-phonon system in a quantum wire and study hot-electron energy relaxation[17] through LO-phonon emission. Although this topic is of great importance by itself,[17] the present purpose is to use it as an example to show the simplicity and the reasonable quantitative accuracy of the plasmon-pole approximation in calculating quantum-wire electronic properties. We, therefore, refrain from discussing in details the hot-electron relaxation phenomena.[18]

When excess energy is supplied to an electron gas, the electrons go out of equilibrium with the underlying lattice, with the electron gas attaining an effective electron temperature T higher than the embedding lattice temperature T_L. Such a hot-electron gas loses energy to its surrounding in order to return to equilibrium with the lattice. In polar semiconductors such as GaAs, the most efficient energy relaxation process, except at very low electron temperatures, is through LO-phonon emission. When reabsorption of the emitted LO-phonons is ignored, the hot-electron energy loss rate at zero lattice temperature is given by[18] (we take $T_L=0$ throughout, our results should be valid for low values of T_L)

$$P=\sum_q \int_{-\infty}^{\infty}\frac{d\omega}{\pi}\omega n_T(\omega)|M_q|^2\mathrm{Im}\chi^{\mathrm{ret}}(q,\omega)\mathrm{Im}D^{\mathrm{ret}}(q,\omega), \tag{21}$$

where $n_T(\omega)$ is the Bose distribution factor at electron temperature T, and $|M_q|^2$ is the Fröhlich coupling matrix.[7] The phonon propagator in Eq. (21) is

$$D(q,\omega)=\frac{2\omega_{\mathrm{LO}}}{\omega^2-\omega_{\mathrm{LO}}^2-2\omega_{\mathrm{LO}}|M_q|^2\chi(q,\omega)}. \tag{22}$$

The last term in the denominator is the phonon self-energy correction due to many-body electron-phonon coupling, which broadens the phonon spectral function. The phonon mode couples to the plasmon excitation (the so-called plasmon-phonon coupling) as well as to particle-hole excitations, so that the renormalized phonon spectrum may be characterized as containing hybridized phononlike and plasmonlike modes, and quasiparticlelike modes. The phononlike mode has a large spectral weight and high energy ($\sim\omega_{\mathrm{LO}}$), while the other modes have small spectral weights but have arbitrarily low energies. At high electron temperatures ($k_BT\sim\omega_{\mathrm{LO}}$), energy relaxation through the emission of the phononlike mode dominates because of its large spectral weight, while at low temperatures ($k_BT\ll\omega_{\mathrm{LO}}$), energy relaxation though emission of the plasmon- and quasiparticle-like modes dominates because of their low energies. The existence of the low energy modes enhances the energy loss rate at low temperatures since emission of bare phonon mode with a frequency ω_{LO} is effectively frozen out when $k_BT\ll\omega_{\mathrm{LO}}$. Our present objective is to compare the energy loss rates among these three cases: no many-body phonon-electron coupling, involving only the bare phonon mode; phonon-electron coupling in the plasmon-pole approximation, involving only the hybridized plasmon- and phononlike modes, but no quasiparticlelike modes; and the phonon-electron coupling in the full RPA, involving all the modes. One can see that these are three increasingly sophisticated approximations to the phonon self-energy correction in Eq. (22) with the phonon self-energy correction completely neglected in the bare phonon case.

With the phonon self-energy ignored, Im$D(q,\omega)$ becomes a single δ-function at $\omega=\omega_{\mathrm{LO}}$. Equation (21) then gives the energy loss rate as

$$P_0=\omega_{\mathrm{LO}}n_T(\omega_{\mathrm{LO}})\sum_q(-2)|M_q|^2\chi(q,\omega_{\mathrm{LO}}). \tag{23}$$

The characteristic of the bare phonon result is an approximate exponential temperature dependence $P_0\propto\exp(-\omega_{\mathrm{LO}}/k_BT)$, which comes from the Bose factor $n_T(\omega_{\mathrm{LO}})$. With the plasmon-pole approximation χ_{PP}, ImD becomes a pair of δ functions at $\omega=\omega_{\pm}$, the frequencies of the hybridized plasmon-phonon modes.[18] The energy relaxation rate is then given as

$$P_{\mathrm{PP}}=P_+ + P_-, \tag{24}$$

with

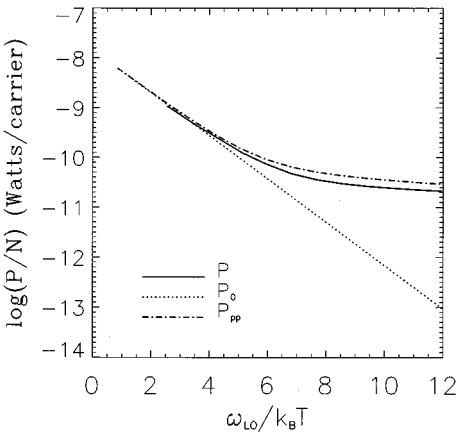

FIG. 4. Energy relaxation rates per electron as functions of electron temperature T. The dotted line, dot-dashed line, and solid line are, respectively, the results with no phonon renormalization, with phonon renormalization in the plasmon-pole approximation, and phonon renormalization in the full RPA. The quantum wire has a carrier density $n=10^5\ \mathrm{cm}^{-1}$ and wire widths $a=b=200$ Å. The base of the logarithmic function is 10.

$$P_{\pm}=\sum_q\ \omega_{\pm}n_T(\omega_{\pm})\frac{\omega_{\mathrm{LO}}|\omega_{\pm}^2-\omega_P^2|}{\omega_{\pm}(\omega_+^2-\omega_-^2)}|M_q|^2(-2)\mathrm{Im}\chi(q,\omega_{\pm}), \tag{25}$$

where $P_{\pm}$ refer, respectively, to energy loss via upper (lower) hybrid plasmon-phonon modes. It should be noticed that the above expression is formally as simple as the corresponding bare phonon result given in Eq. (23), both involving a wave vector integral.

The energy loss rates with no phonon renormalization, with phonon renormalization in the plasmon-pole approximation, and with phonon renormalization in the full RPA, are shown in Fig. 4. Two things need to be emphasized. The first is that the phonon renormalization enhances the energy loss rate by orders of magnitude at low temperatures, although its effect is negligible at high temperatures. The second is that the plasmon-pole approximation gives an excellent description of the energy loss process, in the sense that its result agrees very well with the full RPA result. This example shows again that the plasmon-pole approximation can work remarkably well in a quantum-wire system because of the increased dominance of plasmon excitation in one dimension.

IV. SUMMARY

The plasmon-pole approximation has been widely employed in three- and two-dimensional many-body electron systems. In this work, we discuss two specific applications of the plasmon-pole approximation to 1D electrons in a quantum-wire structure. Our results suggest that the plasmon-pole approximation can work exceptionally well in calculating electronic many-body properties in a semiconductor quantum-wire structure because of the severe phase-space restriction on single-particle electron-hole excitations in one-dimensional systems. We apply the plasmon-pole approximation to calculations of electron self-energy due to Coulomb interactions and hot-electron energy relaxation rate via LO-phonon emission, and find that our calculated PPA results agree extremely well with the results of the full RPA calculations. The agreement of the PPA results with the full RPA results is substantially better (in fact, essentially exact) in 1D than in the corresponding 2D and 3D systems. Our results should influence future electronic calculations in semiconductor quantum wires where calculations may now safely ignore the full complications of the RPA and adapt the simple, intuitively appealing, and quantitatively accurate PPA.

ACKNOWLEDGMENTS

This work is supported by the U.S.-ONR and the U.S.-ARO.

[1] See, for example, *Nanostructure Physics and Fabrication,* edited by M.A. Reed and W.P. Kirk (Academic, Boston, 1989); *Nanostructures and Mesoscopic Systems,* edited by W.P. Kirk and M.A. Reed (Academic, Boston, 1992); C.W.J. Beenakker and H. van Houten, *Solid State Physics: Advances, in Research and Applications,* edited by H. Ehrenreich and D. Turnbull (Academic, New York, 1991), Vol. 44, p. 1; C. Weisbuch and B. Vinter, *Quantum Semiconductor Structures* (Academic, San Diego, 1991).

[2] A.R. Gõni *et al.,* Phys. Rev. Lett. **67**, 3298 (1991).

[3] H. Sakaki, Jpn. J. Appl. Phys. **19**, L735 (1980).

[4] See, for example, D.A.B. Miller *et al.,* Appl. Phys. Lett. **52**, 2154 (1988); S. Briggs, D. Javanovic, and J.P. Leburton, *ibid.* **54**, 2012 (1989).

[5] S. Tomonaga, Prog. Theor. Phys. (Kyoto) **5**, 544 (1950); J.M. Luttinger, J. Math. Phys. **4**, 1154 (1963); D.C. Mattis and E.H. Lieb, *ibid.* **6**, 304 (1965); A. Luther and I. Peschel, Phys. Rev. B **9**, 2911 (1974); F.D.M. Haldane, J. Phys. C **14**, 2585 (1981).

[6] B. Yu-Kuang Hu and S. Das Sarma, Phys. Rev. B **48**, 5469 (1992), and references therein.

[7] Q.P. Li and S. Das Sarma, Phys. Rev. B **43**, 11 768 (1991); **44**, 6277 (1991); E.H. Hwang and S. Das Sarma, *ibid.* **50**, 17 267 (1994).

[8] T. Demel, D. Heitmann, P. Grambow, and K. Ploog, Phys. Rev. B **38**, 12 732 (1988).

[9] B.I. Lundqvist, Phys. Konden. Mater. **6**, 193 (1967); **6**, 206 (1967).

[10] A.W. Overhauser, Phys. Rev. B **3**, 1888 (1971).

[11] L. Hedin and S. Lundqvist, in *Solid State Physics: Advances in Research and Applications,* edited by H. Ehrenreich, F. Seitz, and D. Turnbull (Academic, New York, 1969), Vol. 23.

[12] B. Vinter, Phys. Rev. Lett. **35**, 1044 (1975); Phys. Rev. B **13**, 4447 (1976); S. Das Sarma *et al., ibid.* **18**, 5564 (1978); **19**, 6397 (1979).

[13] David Pines and Philippe Nozières, *The Theory of Quantum Liquids: Normal Fermi Liquids* (Addison-Wesley, New York,

1989); G.D. Mahan, *Many-Particle Physics* (Plenum, New York, 1990).

[14] Q.P. Li, S. Das Sarma, and R. Joynt, Phys. Rev. B **45**, 13 713 (1992).

[15] L. Hedin, Phys. Rev. **139**, A796 (1965); J.J. Quinn and R.A. Ferrell, Phys. Rev. **112**, 812 (1958).

[16] S. Das Sarma and W.Y. Lai, Phys. Rev. B **32**, 1401 (1985); M.A. Stroscio and K.W. Kim, *ibid.* **48**, 1936 (1993); M.A. Stroscio, *ibid.* **40**, 6428 (1989); **10**, 55 (1991); S. Das Sarma and V.B. Campos, *ibid.* **49**, 1867 (1994).

[17] For a review of hot-electron effects in low-dimensional semiconductor structures, see, *Hot Carriers in Semiconductor Nanostructures*, edited by J. Shah (Academic, Boston, 1991).

[18] S. Das Sarma, in Ref. 17.